




# Hybrid multilayered piezoelectric energy harvesters with non-piezoelectric layers

Ramisa Yahyapour<sup>1</sup>, Mohammad Sajad Sorayani Bafqi<sup>1,2</sup>, Masoud Latifi<sup>1,3</sup>, and Roohollah Bagherzadeh<sup>3,4,\*</sup> 

<sup>1</sup>Textile Engineering Department, Textile Research and Excellence Centers, Amirkabir University of Technology, Tehran, Iran

<sup>2</sup>Department of Civil and Industrial Engineering, University of Pisa, Largo Lucio Lazzarino, 56126 Pisa, Italy

<sup>3</sup>Advanced Fibrous Materials LAB, Textile Engineering Department, Institute for Advanced Textile Materials and Technologies (ATMT), Amirkabir University of Technology, Tehran, Iran

<sup>4</sup>College of Materials Science and Engineering, Donghua University (DHU), Shanghai, China

**Received:** 26 May 2021

**Accepted:** 25 October 2021

**Published online:**  
23 January 2022

© The Author(s), under exclusive licence to Springer Science+Business Media, LLC, part of Springer Nature 2021

## ABSTRACT

Fibrous piezoelectric structures as an organic structure constitute a new area of advanced materials for flexible and stretchable sensors and actuators. It is highly desirable to design the structure of piezoelectric generator that the external force can be well-distributed across the entire piezoelectric layer to maximize their power generation. This paper presents a multilayer hybrid structure utilizing electrospun nanofibers and three different materials as passive layers (non-piezoelectric layers) to improve the stress/strain distribution across the piezoelectric layer. Results showed that adding a passive layer could increase the bending modulus of the samples and reduce flexibility. However, they still have the required flexibility to be used in a flexible piezoelectric energy harvester. Under the tapping state, the electrical output of polyvinylidene fluoride (PVDF) nanogenerator devices is highly dependent on the passive layer materials. Furthermore, the results under bending showed that electrical output could be increased using any types of passive layers. It was concluded that adding aluminum, cellulose and polyester as passive layers could increase the electrical output about 4.7, 3 and 4.2 times more than the sample without any passive layer, respectively. Finally, the fabricated nanogenerator showed promising potential for applications such as smart textiles and self-powered wearable devices.

Address correspondence to E-mail: bagherzadeh\_r@aut.ac.ir

## 1 Introduction

The growing demand for smart portable electronics and the batteries problem such as large size, the insufficient capacity, the danger of explosion, and the inconvenience of recharging, has led to the emersion of energy harvesters. Energy harvesters are able to provide long-term power supplies by converting available ambient energies from daily life usage to medical or military applications, such as pressure monitoring systems, implanted sensor nodes, unmanned vehicles, running military security systems, the importance of energy harvesting is increasing progressively. However, in the recent decade micro and nano energy harvesting has become more attention of the researchers [1–3]. Nanogenerators have several groupings and effects such as piezoelectric nanogenerator (PNG), triboelectric nanogenerator (TENG), thermoelectric generator (TEG), and pyroelectric generator (PYG) had been presented in the past decades for a variety of energy harvesting and self-powered uses. The problem with TENGs is that the electrical output is influenced by temperature and humidity [4]. pyroelectric materials are able to generate electrical energy with time-dependent temperature changes. All ferroelectric materials are pyroelectric, and all pyroelectric materials are piezoelectric, but the opposite is not correct. PVDF and its copolymers are used as pyroelectric energy harvesters due to their large pyroelectric constant [5]. Among all energy harvesting methods, electrical energy harvesting from mechanical energy sources is the most attractive and successful method since mechanical movements are independent of ambient conditions and also these ambient energies are mostly accessible [6]. Among the mechanical energy harvesters, piezoelectric materials are the most suitable and effective materials due to their versatility, connectivity, and integration, which are a good choice for using in smart textiles and flexible generators [7, 8]. The on-body demonstration for self-powered sensors is shown in Fig. 1. Common piezoelectric energy harvesters have an energy density of at least three times higher than those of other mechanical energy harvesters such as electrostatic and electromagnetic ones [9]. In order to use piezoelectric harvesters effectively, they should be fabricated from flexible materials instead of brittle piezoceramics.

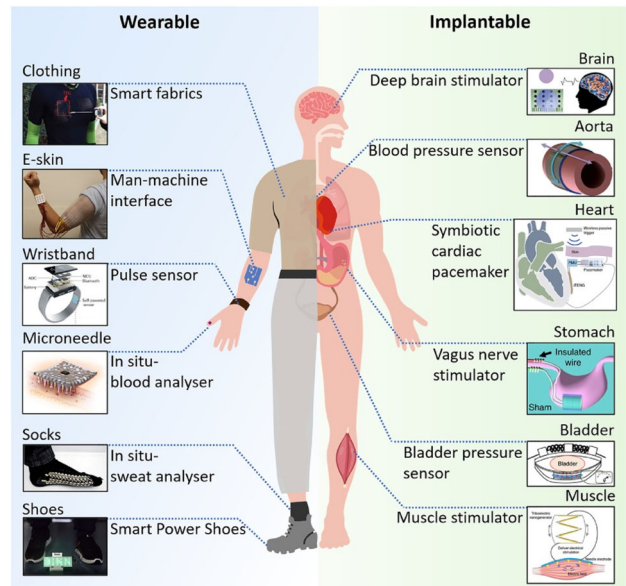


**Fig. 1** On-body demonstration for self-powered sensors (This figure is reused from “Recent progress in human body energy harvesting for smart bioelectronics system” by Yang Zou, Lin Bo, Zhou Li, licensed under CC BY 4.0.) [10]

Piezoelectric materials can generate an electric charge in response to applied mechanical stress; this phenomenon is called the direct piezoelectric effect, which is mostly used in energy harvesters. When a piezoelectric material is exposed under mechanical loading, there will be a replacement in the positive and negative charge centers in the material, which leads to an external electrical field [11, 12]. Piezoelectric effect is reversible, and the indirect piezoelectric effect occurs when an external electrical field causes a stretch or compress on the piezoelectric material [13–15]. Different types of piezoelectric materials are used in industry and technology, but the most popular and usable of them are PZT, BaTiO<sub>3</sub>, and PVDF [16–19]. Piezoelectric polymers are biocompatible, they have the mechanical flexibility and processability into different shapes and can directly be used as an active layer in energy harvesting applications [7, 20]. A commonly used piezoelectric polymer is polyvinylidene fluoride (PVDF) which is used in this study. PVDF is a suitable ferroelectric semi-crystalline polymer with four polymorphs  $\alpha$ ,  $\beta$ ,  $\gamma$ , and  $\delta$  (Fig. 2) [21, 22]. Although the  $\alpha$  phase is the most common and stable phase, the  $\beta$  phase is of great interest due to the highest dipolar moment per unit cell and the largest piezoelectric properties in this phase [23, 24].

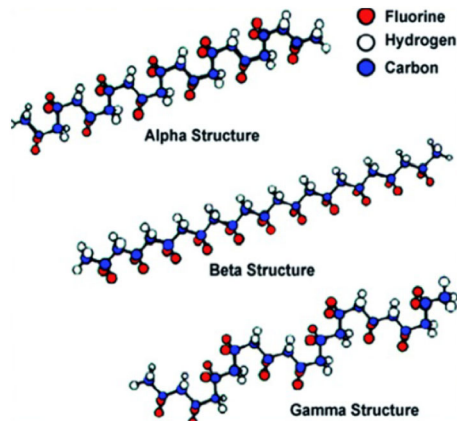


**Fig. 2** Chemical structure of different phases of polyvinylidene fluoride [25]

Piezoelectric devices are the biocompatible and flexible devices with the ability of harvesting energy from both human *in vitro* and *in vivo* motion. The most recent research regarding different possible structures and designs of piezoelectric energy harvesters using for self-powered and wearable electronics are smart footwear, smart textile and smart skin. By contrast piezoelectric nanogenerators are known as a capable green energy harvesting technique [26]. In 2018, Talbourdet et al. investigated the differences between 2 and 3D woven fabrics from 100% optimized piezoelectric PVDF multifilament yarns. The textile structures were poled after the weaving process, and a maximum output voltage of 2.3 V was observed on 3D woven under compression by DMA tests. It was found that the 3D interlock design could improve energy harvesting due to the stresses of the multifilaments in the thickness [27].

In 2020, a thin polymeric film based on poly(vinylidene fluoride-co-hexafluoropropylene) (PVDF-HFP) and poly(methyl methacrylate) PMMA was used for energy harvesting by Polat. The results showed that blending with PMMA could increase the  $\beta$ -phase content and improved the heat stability. 84.7% increase found in the piezoelectric potential could be a favorable result for energy harvesting and sensors applications [3].

The list of developed piezoelectric generators in the similar works is reported in Table 1. It should be considered that different loading situations and sample dimensions lead to variety of output.

The invention of piezoelectric generators provides a new procedure for powering portable electronic devices with low-energy consumption [36]. They can

operate under stress or strain, such as arm twisting, knee bending, and expansion of the lungs and abdomen while breathing. Thus, a flexible piezoelectric substrate is a common choice for these environments [37]. It is clear that piezoelectric polymers (such as PVDF) are naturally flexible, and they are the preferred option for flexible harvesters. However, low power output is the main impediment of scavenging energy from a polymeric piezoelectric material that can be reached only in a specific frequency.

Furthermore, ambient energies usually exist at the low-frequency range and the low-frequency vibration sources such as human motions. It means that the electrical energy from these ambient sources has low amplitudes. Therefore, many approaches have been taken different strategies to improve the performance of piezoelectric energy harvesters at low-frequency [38, 39].

Piezoelectric materials are mostly bonded on a substrate and built in a rectangular cantilever shape. The more piezoelectric material cannot guarantee the efficiency of a harvester, and many studies have been done to improve the output power by modifying the geometry and the structure of energy harvesters [40–42]. The number of the piezoelectric layers and the type of electrode connection are other important parameters that influence the performance of an energy harvester [43]. It is reported that a multilayer bimorph energy harvester produces more power output at the same frequency and total thickness [44–46]. Other researches conducted in this field showed that, by increasing the number of layers, a small reduction of power output occurred, but the thickness of electrodes can explain this reduction. The theoretical analysis omitted the increases of electrode thickness, leaving the material volume unaffected [47]. The main factor of designing the structure of a piezoelectric generator is to maximize the applied stress or strain of an external load on the piezoelectric layer [48, 49]. This point is specifically crucial for a flexible piezoelectric generator. Because of the inherent softness of the matter, especially while bending, the stress or strain response may be concentrated which can, in turn, limit the amount of the electricity produced by the piezoelectric matter [50, 51].

There have been different endeavors to achieve high power output, such as different designs, non-linear methods, optimization techniques, and harvesting materials. In some works, the effect of

**Table 1** The comparison of different polymeric piezoelectric energy harvesters

Piezoelectric material	Passive layer material	Sample size	Loading conditions	Output voltage	Other electrical parameters	Refs
PVDF film (commercial)	Without passive layer	2 × 7 cm	Mechanical stretching up to 800 mN	16.4 V (peak-to-peak)	0.2 μA/cm <sup>2</sup> (peak-to-peak)	[28]
Multilayer PVDF film	Silicone rubber	8 × 5 cm		136 V (peak-to-peak)		[29]
PVDF-TrFE film	Kapton	2 × 0.4 cm	Repeatable strain of 0.103%	2 V (peak)	300 nA (peak)	[30]
PVDF film (Mg salt filler)	PDMS	36 × 20 mm		5 V (peak-to-peak)		[31]
PVDF-TrFE film	PEN	1 cm <sup>2</sup>	Bending strain of 0.081%	8 V (peak-to-peak)	0.8 μA/cm <sup>2</sup> (peak-to-peak)	[32]
PVDF-TrFE film (solvent annealed)	PET		Pressure Applied with a weight of 25 g/cm <sup>2</sup> at 3 Hz	11 V (peak-to-peak)	0.6 μA (peak-to-peak)	[33]
PVDF-TrFE film	Kapton	0.09 cm <sup>2</sup>	strain of 0.943% at strain rate of 4.441% s <sup>-1</sup> at 0.75 Hz	7 V positive peak	58 nA positive peak	[34]
PVDF-TrFE film (with grapheme oxide)	Without passive layer	1 cm <sup>2</sup>	Compression pressure of ~ 0.32 MPa applied at 1 Hz frequency	4.3 V (peak)	1.88 μA (peak)	[35]

electrodes on a membrane energy harvester was considered. The results showed that electrode coverage of 60% revealed the best electromechanical coupling [29].

Optimizing the thickness was launched by Paquin and Amant, who suggested a semi-analytical model based on the Rayleigh–Ritz approximations [47]. In 2014, Zhao and You designed a 1 mW shoe-embedded PVDF energy harvester. For higher power output, the authors accumulated eight layers of PVDF films together and sandwiched them between two wavy surfaces. Under quick walking at ~ 1 Hz, a peak-to-peak voltage of 136 V, a peak power of 4 mW, and average power of 1 mW were obtained [9].

In 2015, a pair of PVDF-PI composites was assembled back to back to form a curved PVDF energy harvester by Jung et al. An arc-shaped polyimide (PI) substrate with a thickness of 0.2 mm was used and on each side of it, two 0.1 mm thick PVDF films were attached. In this formation, while loading, PVDF films experience bending stress without stretching. The sample was fabricated with four 70 × 40 mm<sup>2</sup> PVDF films, which generated an averaged open-circuit voltage of 25 V at 0.5 Hz. The high efficiency of this harvester was due to the large surface area

(multiple layers) and the high bending stress of the curved structure [5]. Furthermore, there were several examples of using non-piezo materials in energy harvesters. A “3D spacer” was demonstrated with the silver-coated polyamide multifilament yarn layers electrodes, and the spacer yarns were high β-phase PVDF monofilaments which provided a maximum power density of 5.07 μW/cm<sup>2</sup>.

Therefore this study attempts to present a multi-layer hybrid structure including both piezoelectric (electrospun PVDF micro-nano fibers) and non-piezoelectric layers, called passive layer in this article, that has the required flexibility and at the same time, it produces proper output. The microstructural, crystalline structural, mechanical and thermal properties of the electrospun PVDF were investigated using the scanning electron microscope, X-ray diffraction, Fourier transform infrared spectroscopy, Instron instrument, and differential scanning calorimetry, respectively. An instrument called PiezoTester was manufactured for piezoelectric properties evaluation and electrical output measurement. The influence of the passive layer factors such as thickness, shape, and material on the electrical output was studied under bending and tapping load. The

bending modulus of the prepared harvesters was measured to find a relation between bending modulus and electrical output. The difference between this work and the other reports is that they were based on improving the piezoelectric materials and output. However, this study aims to develop a new structure to improve the performance of the harvesters. In order to increase the power output, the mechanical damping effect of energy harvesters should be minimized.

## 2 Experimental section

### 2.1 Materials

Polyvinylidene fluoride polymer [PVDF; molecular weight (mW) 230000] was purchased in granule form from Halopolymer Company. Acetone (99%) and *N,N*-dimethylformamide (DMF, 99%) were purchased from Merck Company. Aluminum foil was used as electrodes. Cellulose, polyester, and aluminum layers were used as passive layers with different thicknesses.

### 2.2 Electrospinning

To produce piezoelectric fibers, electrospinning equipment with a rotary drum was used (Fig. 3). PVDF solution (26 wt/wt%) was prepared by dissolving PVDF granule in an acetone/DMF solvent mixture (2/3 wt/wt) and then the mixture was stirred with a magnetic stirrer for 2 h at 60° C. Finally, a clear solution was obtained.

Nanofibrous layers were fabricated using the FNM© electrospinning system. Feeding rate, applied voltage, and the collector rotating speed were selected according to the previous studies [7, 52]. Based on the aforementioned proper conditions, the spinning distance (collecting distance) was considered 18 cm.

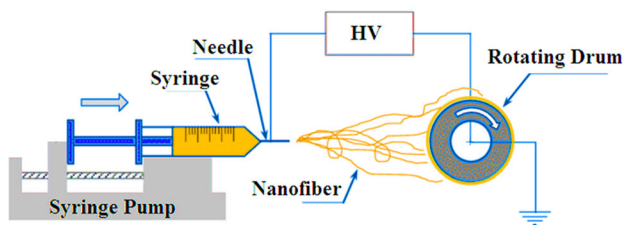


**Fig. 3** Schematic view of the electrospinning setup used to fabricate PVDF nanofiber layers

A syringe with a volume of 1 ml and a needle with a gage of 22 (needle length 34 mm, inner diameter 0.4 mm and outer diameter 0.7 mm) were used in electrospinning. The spinning solution was loaded into a syringe and pumped with the flow rate at 0.5 ml h<sup>-1</sup>. An 18 kV voltage was applied between the needle and the drum collector.

### 2.3 Preparation of piezoelectric devices

After fabricating the fiber layers, the samples were prepared in combination with the passive layer, according to Table 2 and Fig. 4, for bending and electrical output tests. The samples for electrical output tests were prepared in two different forms.

The specimens were prepared in 2 × 2 cm for tapping tests and in 1 × 5 cm for bending tests. Cardboards in different thicknesses were used as available cellulose layers, PET films were used as polyester layers, and aluminum foils were used as aluminum layers. The reason for using the aluminum layer as one type of passive layers was to investigate the influence of a conductive passive layer on the performance of the harvester.

### 2.4 Characterization

Shirley fabric thickness tester (mode: SDLO 34 with 0.01 mm accuracy) was used for measuring the thickness of produced passive layers based on ASTM D1777-96. To investigate the morphology of the produced micro-nano fiber layers and to ensure their uniformity, a scanning electron microscope (SEM, Philips Model XL30) was employed. The diameter of micro-nano fibers was measured by Image-J software. One hundred fibers were measured to calculate the mean fiber diameter for each sample. For crystal structure analysis, X-ray diffraction (XRD) was used (Equinox3000, INEL Company—Cu, K<sub>α</sub>: 0.154 nm). Differential scanning calorimetry (DSC) was used to study the thermal properties and crystal structure of the electrospun micro-nano fibers using a DSC2010 TA instrument Co. Fourier transform infrared spectroscopy (FTIR) analysis was carried out on the layers by FTIR spectrometer (NEXUS 670, Nicolet Company). The bending behavior of the samples was measured by an Instron 5566 Universal Testing System instrument according to ASTM E855 standard, at the displacement rate speed of 1 mm min<sup>-1</sup>. For this purpose, suitable and movable support was first

**Table 2** Sample naming based on thickness and used material

Samples	Passive layer material	Passive layer thickness ( $\mu\text{m}$ )	Final sample thickness ( $\mu\text{m}$ )
S1	Without passive layer	0	100
S2	Aluminum	30	130
S3	Aluminum	120	220
S4	Aluminum	420	520
S5	Cellulose	120	220
S6	Cellulose	420	520
S7	Polyester	120	220
S8	Polyester	420	520

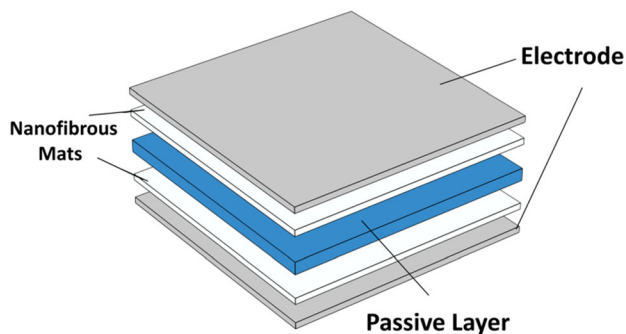


**Fig. 4** Schematic view of the structure of the samples. The thickness of a nanofiber layer and embedded aluminum foil is 50 micron

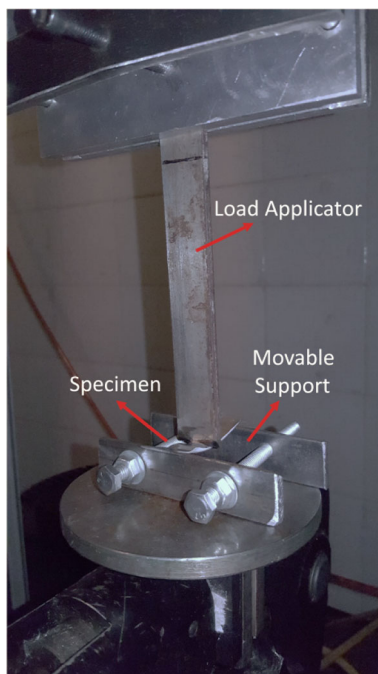


**Fig. 5** A view of manufactured support used to measure the bending rigidity of the samples

designed and manufactured according to the above standard and then mounted on the machine (Fig. 5).

A homemade instrument called PiezoTester system was used (<http://ffm.aut.ac.ir>) to evaluate the piezoelectric properties and to measure the electrical output of the harvester [53]. This evaluation was performed in both tapping and bending modes. To do this test, from each sample, 5 specimens were evaluated and the mean value was reported.

### 3 Result and discussion

Since the same electrospun layer was used for all samples, the active layer parameters were discussed first.

#### 3.1 The electrospun fiber layer morphology

Achieving a uniform piezoelectric property comes from the production of uniform and beadless micro-nano fibers. Therefore, uniform production of micro-

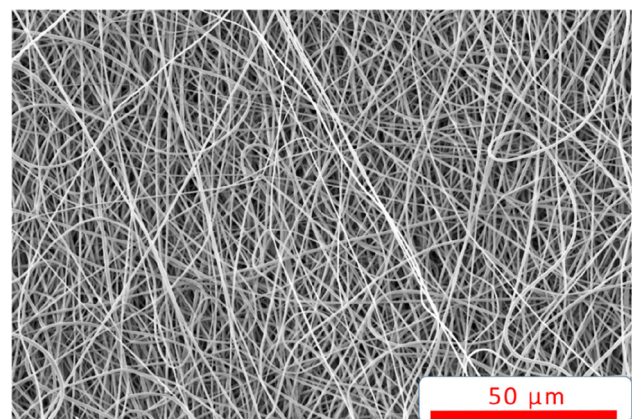


**Fig. 6** The SEM image of a prepared sample. Fabrication parameters are: Distance: 18 cm, Applied voltage: 18 kV, Feed rate: 0.5 ml/h and Rotating speed: 400 rpm. The average diameter of the nanofiber is 620 nm

nano fibers must be ensured. As can be seen in the SEM image shown in Fig. 6, the fabricated micro-nano fiber layers were homogeneous and beadless, so it can be stated that the electrospun fiber layer has the required uniformity to be used in a piezoelectric harvester.

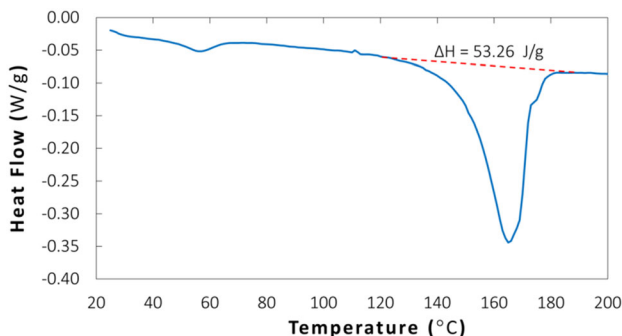
### 3.2 Crystallinity

Among all crystalline phases in PVDF polymer, the beta phase is the most appropriate one for piezoelectric properties. The electrospun fiber layer was first subjected to DSC thermal analysis to determine its crystallinity, and then based on the acceptable range in the related articles; further evaluations were carried out. To calculate the degree of crystallinity for each sample, Eq. (1) was used.  $X_c$  indicates the degree of crystallinity of the sample and  $\Delta H_{lit}$  is the melting enthalpy for the state where the material is 100% crystalline in the beta phase [54].

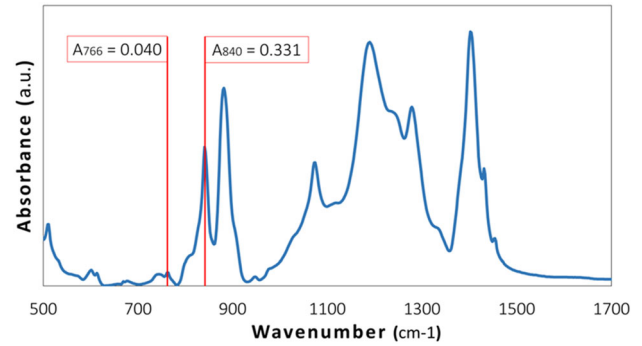
$$X_c = \frac{\Delta H_{m(Sample)} \times 100}{\Delta H_{lit}}, (\Delta H_{lit} = 103.4 \frac{J}{g}) \quad (1)$$

Figure 7 shows the DSC spectrum for the electrospun mats. By measuring  $\Delta H$  (with the help of TA Universal Analysis software) and placing it in the Eq. (1), the percentage of crystallinity of the fiber layer was calculated to be about 51.4%, which is in the appropriate range.

After thermal analysis, FTIR spectroscopy was used to investigate the structure of the produced micro-nano fibers and calculate the beta phase crystallinity ratio of the entire crystal structure. The diagram of the performed test on the electrospun fibrous mat is shown in Fig. 8. To determine the crystallinity of the beta phase in each sample, the absorption



**Fig. 7** The DSC test diagram of the fabricated layer.  $\Delta H_m$  is  $53.26 \text{ J.g}^{-1}$



**Fig. 8** FTIR spectroscopy of the PVDF micro-nano fiber layer

spectral peaks of the alpha and beta phases were evaluated at  $766$  and  $840 \text{ cm}^{-1}$ , respectively. The beta phase of the crystal was calculated from Eq. (2):

$$f(\beta) = \frac{X_\beta}{X_\beta + X_\alpha} \times 100 = \frac{A_\beta}{1.26A_\alpha + A_\beta} \times 100 \quad (2)$$

where  $A_\alpha$  and  $A_\beta$  are absorptions at  $766$  and  $840 \text{ cm}^{-1}$  for alpha and beta phases, respectively, and  $X_\alpha$  and  $X_\beta$  are crystallinity degrees for alpha and beta phases, respectively [55]. These values were extracted using OMNIC software and placed in Eq. (2). As shown in Table 3, 87% of the crystalline part is in the beta phase.

X-ray diffraction (XRD) was used as another crystal structure test to confirm and monitor the results obtained from FTIR and DSC experiments. As mentioned, the piezoelectric property of polyvinylidene fluoride polymer, results from the beta phase of its crystal structure. The presence of a spectral peak at an angle of  $2\theta = 20.5$  in the X-ray diffraction spectrum of this polymer indicates the beta phase in its crystal structure. Also, the presence of a spectral peak at an angle of  $2\theta = 18.5$  indicates the alpha phase of the crystal structure [54]. As shown in Fig. 9, the spectral peak intensity at  $20.5^\circ$  is much higher than the spectral peak intensity at  $18.5^\circ$ , indicating that the beta phase is formed in the electrospun fiber layer. This is in confirmation of the results of the DSC and FTIR experiments.

**Table 3** FTIR spectroscopy results

Wavenumber absorption intensity		$f(\beta)$
$A_{766}$	$A_{840}$	
0.040	0.331	87%

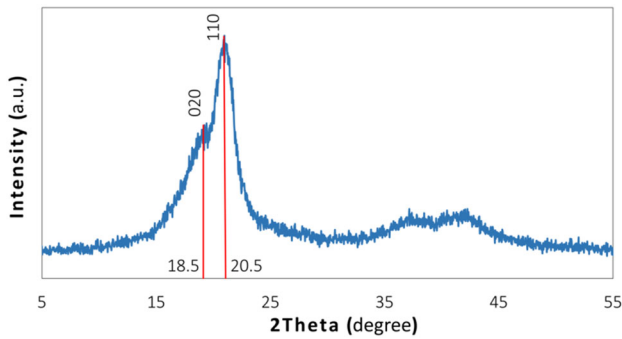


**Fig. 9** XRD diagram of the micro-nano fibrous layer

The crystallite size was estimated from the Scherrer Eq. (3) [56],

$$D = \frac{K\lambda}{\beta \cos\theta} \quad (3)$$

where  $D$  is the average crystallite size,  $\lambda$  is the x-ray wavelength,  $\beta$  is the width of the x-ray peak on the  $2\theta$  axis, normally measured as full width at half maximum (FWHM) after the error due to instrumental broadening has been properly corrected (subtraction of variances),  $\theta$  is the Bragg angle, and  $K$  is the so-called Scherrer constant [57]. The constant  $K$  has been determined to vary between 0.89 and 1.39, but it is usually taken as close to unity, the assumption that  $K = 1.0$  is generally justifiable [56]. At the  $2\theta$  value of 20.5, calculation has produced crystallite size is 5 nm.

All the above experiments proved that the fabricated layers have proper piezoelectric properties to consider them as active layers in the energy harvester devices. In the next step, the effect of passive layers on bending rigidity and electrical output was evaluated.

### 3.3 Bending rigidity

In order to study the effect of the passive layer on bending strength and flexibility of the produced specimen, a three-point bending test was performed based on the ASTM E855 standard. In this experiment, the bending modulus and the stress–strain response of the material were determined under bending loading. During the experiment, there was a compressive stress in the upper surface (above the neutral axis) and tensile stress in the lower one. Figure 10 shows a diagram of the sample in which the vertical axis represents the force and the horizontal axis represents the displacement.

The bending modulus of each sample was calculated from diagrams (the slope of the first 5% of the diagram) and shown in Table 4 and Fig. 11. As can be seen, by adding a passive layer, the bending modulus of the samples was increased. This improvement in modulus increased with raising the passive layer thickness so that the modulus of S4 is more than 6 times higher than that of S1. In the samples with the same thickness of the passive layer, the aluminum layers had the highest modulus increase and the samples with the cellulose layer had the lowest modulus growth.

In other words, adding a passive layer can reduce flexibility. This decrease in flexibility of the nano-generator device is in its maximum for the S4 and then S8. ANOVA test was performed and the results showed that this difference between the flexibility of samples is significant (Supplementary data—SD1).

### 3.4 Electrical output

Due to the direct piezoelectric effect, if mechanical stress is applied to a piezoelectric material, an electrical response is obtained. For this reason, one of the important methods to evaluate the piezoelectric properties and performance of an energy harvester is to apply mechanical stress to the sample and measure its electrical output [55]. The experiment was performed on the samples in two different ways. In the first method, the specimens were subjected to a tapping load with a given force and frequency, and their electrical output was measured. In the second method, the specimens were subjected to a periodic bending force with a 5 mm displacement and their output was recorded. Since the ultimate goal is to use these harvesters in smart textiles and especially in garments that the applied load is in bending mode, the second method was considered.

#### 3.4.1 Tapping mode of evaluation

To evaluate the piezoelectric properties of the manufactured samples, their electrical output was measured under a specified load and at a specified frequency. For this purpose, 5 specimens from each sample were prepared in  $2 \times 2$  cm, with the thickness and arrangement mentioned in Table 2, and they were subjected to a 2.65 N tapping load with a frequency of 5 Hz. The average output value of each sample is shown in Table 5 and Fig. 12. ANOVA test



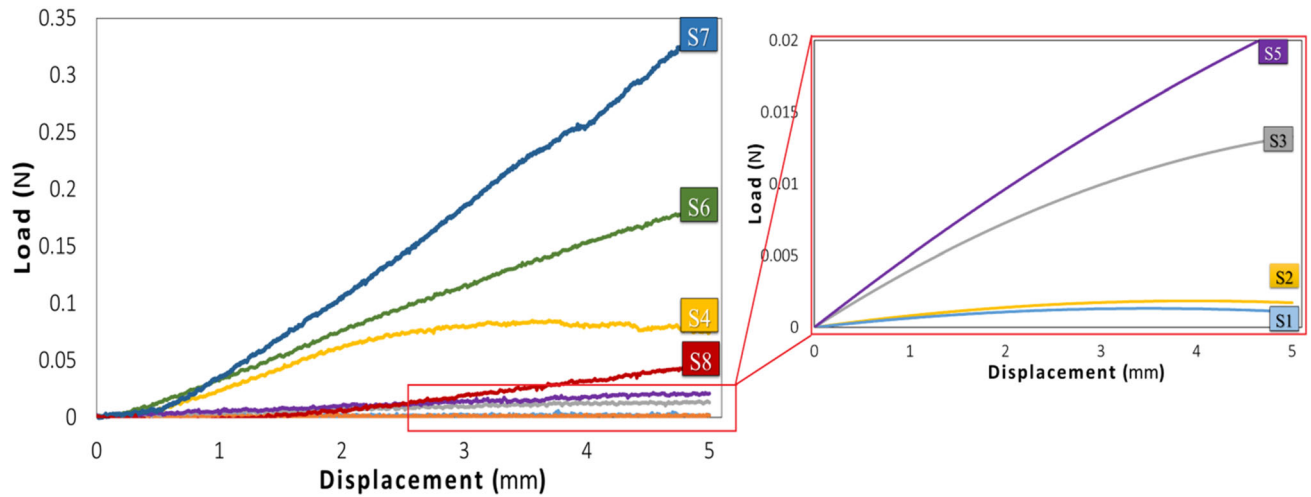


**Fig. 10** Bending load versus displacement diagram of samples

**Table 4** Bending modulus of samples

Samples name	Bending modulus (KPa)	CV%
S1	125	21
S2	337	18
S3	585	14
S4	1797	7
S5	578	14
S6	917	12
S7	722	17
S8	1425	10

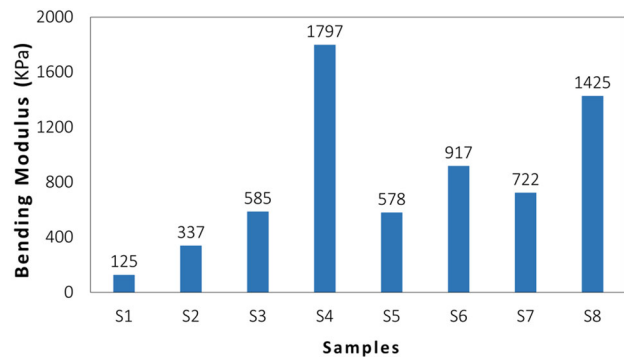


**Fig. 11** Variation of bending modulus in different samples

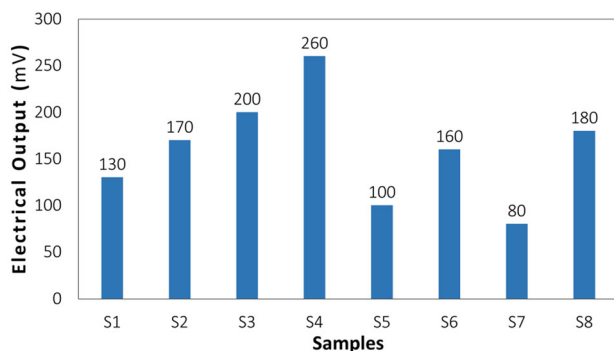
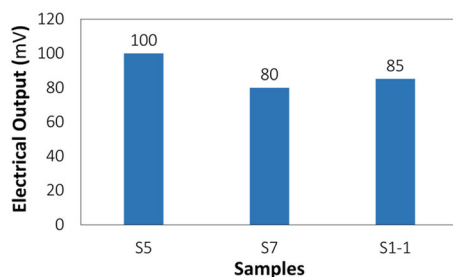
was performed and the results showed that the data were significant (Supplementary data—SD2).

**3.4.1.1 Passive layer material** As shown in Fig. 12, adding a passive layer causes a noticeable change in the electrical output of the fabricated nanogenerator device. Nevertheless, this change varies depending

on the material of the passive layer. By comparing S1 to S4, it can be claimed that the amount of power output increased with the addition of the passive layer. However, in S5 compares to S7 and S6 compares to S8, adding the passive layer has a different trend so that in S5 and S7, the output is even lower than S1. As the thickness increases from 120 to 420 microns, the output value is increased in all three passive layers. The reason for the decrease in the electrical output in S5 and S7 can be attributed to the passive layer mechanical energy absorption, which is caused by the applied force. So less energy is transferred to the lower piezoelectric layers of the active layer and then the electrical output is reduced. In other words, it can be claimed that in practice, only one layer of nanofibers is effectively active in generating electrical energy. To investigate this claim, S1-1 with the same structure as S1 but with a monolayer of nanofiber was produced and tested. As can be seen in Fig. 13, the outputs of S5 and S7 are up to 20% higher than that of S1-1 and are not significantly different while their active layer content is 2 times higher. This result can be considered as a confirmation of the above claim that only one layer of nanofibers is effectively active in generating electrical energy. This effect is not observed in the samples with the aluminum passive layer because not only they are elastic, but also they have very low-energy absorption and are able to transfer energy from one side to the other. ANOVA test was also performed and the results showed that the data were not significant, confirming the damping claim (Supplementary data—SD3).

**Table 5** Piezoelectric response of samples under tapping mode loading

Type of loading	Sample	Output (mV)	Sensitivity (mV/N)	CV%
Tapping	S1	130	49.05	12
	S2	170	64.16	10
	S3	200	75.47	11
	S4	260	98.11	13
	S5	100	37.74	11
	S6	160	60.38	12
	S7	80	38.19	20
	S8	180	67.92	11

**Fig. 12** Electrical output diagram under tapping mode loading**Fig. 13** The effect of the passive layer material on electrical output

**3.4.1.2 Passive layer thickness** As can be seen in Fig. 12, in all 3 passive layer types, as the thickness of the passive layer increases, the electrical output increases and the sample outputs follow the same trend for all 3 types. In other words, it can be stated that by increasing the thickness (in specific material), the electrical output increases.

An essential point in the trend of output changes can be seen in the comparison of S6 and S8. As explained in the previous section, by adding a passive layer, the applied force is absorbed by the passive layer and is not transferred entirely to the bottom layer. However, with increasing the layer thickness, which is associated with increased energy absorption

(increased viscoelastic effect), the output value is increased. At first sight, this is inconsistent with the above claim. This issue can be justified by two different perspectives, which are based on the capacitive property and device measuring mechanism. These two explanations are discussed as follow:

**3.4.1.3 Explanation based on the capacitive property** As shown in Fig. 4, the samples are in fact capacitors consisting of two conductive aluminum plates and a multilayer dielectric. The following equations generally describe capacitors:

$$C = q/V \quad (4)$$

$$C = \epsilon A/d \quad (5)$$

where  $C$  is the capacitance,  $q$  is the charge stored in the capacitor,  $V$  is the voltage across the capacitor,  $A$  is the common plane of the two capacitors,  $d$  is the distance between plates, and  $\epsilon$  is the dielectric coefficient of the non-conductive layer between the two plates. Since the thickness of the piezoelectric nanofiber layer is the same in all the samples and assuming the applied force as constant, the induced charge in the samples can be considered the same ( $q_1 = q_2$ ).

On the other hand, the dielectric coefficient is the same in the samples with the same passive layer ( $\epsilon_1 = \epsilon_2$ ). All samples were also prepared in a similar size ( $A_1 = A_2$ ). With these points in mind, it can be written:

$$\begin{aligned} (4) \quad \frac{C_1}{C_2} &= \frac{V_2}{V_1} \\ \Rightarrow C_2 &= \frac{V_1}{V_2} C_1 \end{aligned} \quad (6)$$

$$\begin{aligned} (5) \quad \frac{C_1}{C_2} &= \frac{d_2}{d_1} \\ \Rightarrow C_2 &= \frac{d_1}{d_2} C_1 \end{aligned} \quad (7)$$

$$\begin{aligned} (6),(7) \quad \frac{V_2}{V_1} &= \frac{d_2}{d_1} \Rightarrow V_2 = \frac{d_2}{d_1} V_1 \end{aligned} \quad (8)$$

According to Eq. (8), with increasing thickness, the potential difference between the two samples increases. In fact, assuming constant load created in the samples by increasing the passive layer thickness, the potential difference of the samples increases.

**3.4.1.4 Explanation based on the device measuring mechanism** In the PiezoTester method, as shown in Fig. 14, the force sensor is located precisely below the sample and measures the force applied to the sample. On the other hand, as mentioned above, the applied force is the same for all the samples and equals 2.65 N. It is conceivable that in this measurement system, the amount of force is not predetermined and the applied value is measured after applying force to the sample by the below sensor. When it is stated that the force is 2.65 N, it means that the force applied to the sensor is 2.65 N.

Since the samples have viscoelastic properties, the actual applied force is higher than this. The more viscoelastic the sample, the greater the difference between the measured force and the actual applied force is. When the passive layer thickness increased or, in other words, the viscoelastic effect of the samples becomes more significant, it is necessary to give more force to the samples with thicker passive layers than to the thinner layer samples so that the sensor can sense a constant force of 2.65 N. The higher the force, the more mechanical energy enters the upper piezoelectric layer, which results in the higher piezoelectric output. In fact, the increase in the output observed in S8 and S6 compared to S7 and S5, and even S1 is due to the increase in the applied force to the upper piezoelectric nanofiber layers during the measurement.

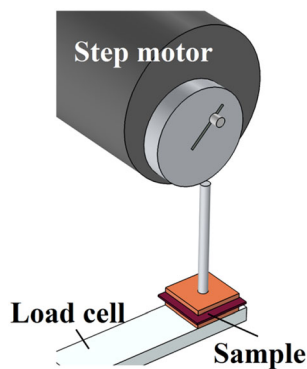


Fig. 14 Schematic view of PiezoTester

**3.4.1.5 Effect of passive layer geometry on the electrical output** In order to investigate the effect of the geometry of the passive layer on the electrical output of the piezoelectric devices, S2-2 was produced using a netted aluminum foil to place between the two piezoelectric layers similar to the S2 layout, and its electrical output was evaluated (Fig. 15).

As can be seen in Fig. 16, the spectral peak intensities of each sample are approximately the same and the outputs are in equal magnitude. Therefore, it can be stated that passive layer with the selected geometry has little effect on the electrical output of multilayered piezoelectric devices. ANOVA test was performed and the results showed that the data were not significant (Supplementary data—SD4).

**3.4.2 Bending mode of evaluation**

Since one of the most important applications of energy harvesters is the use in smart textiles and bending is one of the major deformations available in this application, piezoelectric property evaluation of the samples was also performed in bending mode. For this purpose, 5 samples, 5 × 1 cm, were produced with the arrangement mentioned in Table 1.

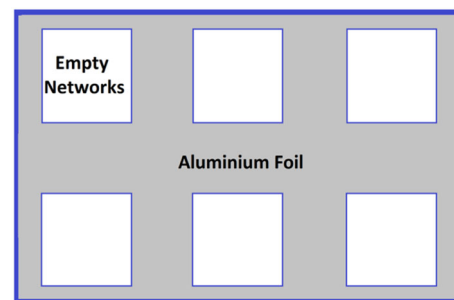


Fig. 15 The netted aluminum layer used as a passive layer

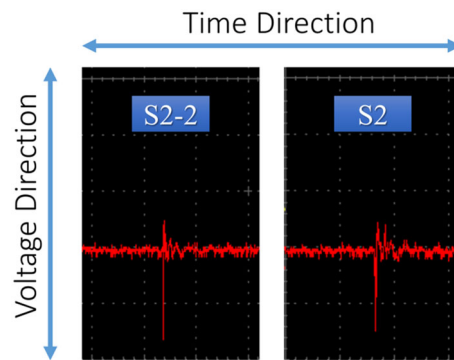


Fig. 16 Electrical output spectra of sample S2 and S2-2

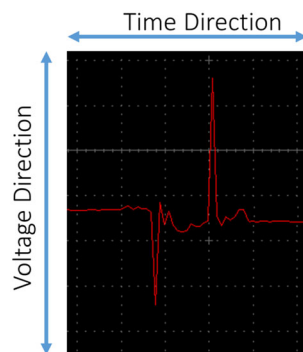
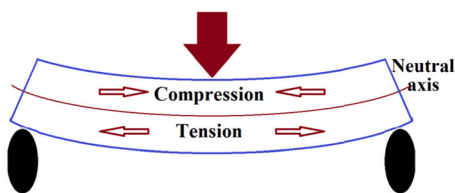
**Table 6** The average electrical output of the samples under bending loading

Sample	Output in loading (V)	CV%	Output in unloading (V)	CV%
S1	0.8	31	0.6	41
S2	2.2	17	1.4	18
S3	2.6	11	1.8	16
S4	4.6	12	1.4	17
S5	2.6	17	2	19
S6	3.2	14	2.4	18
S7	2.8	11	2.4	10
S8	4.2	8	3.6	7

The average electrical output of the samples is shown in Table 6.

Since each bending period consists of two loading and unloading stages, electrical output was observed at each step (Fig. 17).

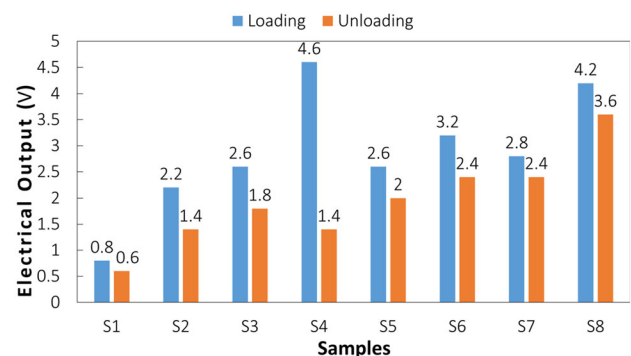
Figure 19 shows the mean electrical output under bending. As can be seen, by adding a passive layer, the electrical output increases in all devices with three types of passive materials. As the thickness of the passive layer increases, the electrical output increases. The reason for this can be attributed to the increase in the bending modulus of the samples. Another factor that increases the output is the increasing distance of the piezoelectric layer from the neutral axis with increasing the thickness. Every material under bending is divided into two parts (Fig. 18). In the upper part from the neutral axis, the

**Fig. 17** Electrical output spectra under bending loading**Fig. 18** The behavior of the structure under bending loading

structure is under a compressive force, and in the lower part from the neutral axis, the structure is under a tensile force. The higher the distance from the neutral axis, the greater effect of forces is expected. As the thickness of the passive layer increases, the distance from the neutral axis increases, and this factor extends the piezoelectric output.

Besides, checking the Fig. 19 shows that the electrical output under loading is higher than the electrical output under unloading. The reason for this can be attributed to the fact that loading takes place under force, and unloading takes place inactively and without any external force. In this case, the ability to return to the original state is important.

As shown in the diagram, in the sample consist of polyester layer, due to better reversibility, the unloading output is higher than the ones made from cellulose or aluminum. However, in the aluminum sample, since the sample experiences plastic deformation after loading (no returns), the unloading output is smaller. ANOVA test was performed and the results showed that these results were significant (Supplementary data—SD2).

**Fig. 19** The electrical output of samples under bending load

## 4 Conclusion

Nowadays, portable energy harvesters with extensive life span have grown for a wide range of applications. It is very likely that batteries will be removed from miniature devices in near future. This study introduced a new structure which can be directly integrated in potential wearables to charge portable electronics through body movements or even be used as a flexible and reliable power supplies. It is clear that the output voltage of the PVDF piezoelectric devices depends on the volume of material, and the amount of applied stress, the two factors that should be considered when designing a flexible piezoelectric assembly. On the other hand, the key aspect of designing a piezoelectric harvesting structure is to maximize the stress or strain created on the piezoelectric substrate by applying an external force. When the external force is applied in the middle of a PVDF film without a passive layer, it pushes the surface straight down, causing it to locally bend due to its large flexibility. However, the hybrid structure enables the PVDF to uniformly increase the applied stress on the entire surface of the material. In this status, the amount of electricity produced by the material is limited.

The results showed that under the tapping state, the electrical output of PVDF nanogenerator devices is highly dependent on the materials of the passive layer. If the passive layer is a high-energy-absorbing viscoelastic material, the addition of this layer has adverse effects, which decrease the electrical output comparing with the low-energy-absorbing materials.

Nevertheless, if a rigid layer capable of transmitting force is used, the addition of the passive layer increases the electrical output, and increasing its thickness leads to higher output. However, the bending test results showed that the use of such a layer has a limitation on device flexibility. The result of electrical output under bending was slightly different. These results showed that the addition of a passive layer increased the electrical output in all three materials and all thicknesses. As the thickness of the passive layer rises, the output also increases. Besides, if the sample is produced from a flexible and elastic passive layer, its output is similar under loading and unloading, and the output has a higher uniformity. Finally, it can be stated that the passive layer is more suitable in the harvesters under bending. It was concluded that adding aluminum,

cellulose and polyester as passive layers could increase the electrical output about 4.7, 3 and 4.2 times more than the sample without any passive layer, respectively. In this case, the use of elastic passive layer is preferable comparing with the cellulose and aluminum layers. In the case that the nanogenerator is subjected to a tapping loading, the use of the passive layer is not justified and is only recommended if a rigid layer is used.

Thus, it seems that the number of applications will be increased in future. Efforts should be done to improve the performance of energy harvesters by fabricating new piezoelectric materials and composites. Optimizing the conditions to attain a high power output and a wide working bandwidth are the two goals which should be considered more in the future.

## Acknowledgements

The support provided by the ATMT Institute, Department of Electrical and Computer Engineering, Deakin University, University of Donghua, and INSF (Grant No 97016813) are highly appreciated.

## Declarations

**Conflict of interest** There are no conflicts to declare.

**Supplementary Information:** The online version contains supplementary material available at <http://doi.org/10.1007/s10854-021-07296-1>.

## References

1. Vivekanathan, V., et al., Triboelectric Nanogenerators: Design, Fabrication, Energy Harvesting, and Portable-Wearable Applications, in *Nanogenerators*. 2020, IntechOpen.
2. P. Costa et al., Recent progress on piezoelectric, pyroelectric, and magnetoelectric polymer-based energy-harvesting devices. *Energy Technol.* **7**(7), 1800852 (2019)
3. K. Polat, Energy harvesting from a thin polymeric film based on PVDF-HFP and PMMA blend. *Appl. Phys. A* **126**, 1–8 (2020)
4. F. Narita, M. Fox, A review on piezoelectric, magnetostrictive, and magnetoelectric materials and device technologies for energy harvesting applications. *Adv. Eng. Mater.* **20**(5), 1700743 (2018)

5. M.S. Bafqi, R. Bagherzadeh, M. Latifi, Nanofiber alignment tuning: An engineering design tool in fabricating wearable power harvesting devices. *J. Ind. Text.* **47**(4), 535–550 (2017)
6. H. Liu et al., A comprehensive review on piezoelectric energy harvesting technology: materials, mechanisms, and applications. *Appl. Phys. Rev.* **5**(4), 041306 (2018)
7. Bafqi, M.S., et al., Design and fabrication of a piezoelectric out-put evaluation system for sensitivity measurements of fibrous sensors and actuators. *J. Ind. Text.*, 2019: p. 1528083719867443.
8. Y. Zhang et al., Ferroelectric and piezoelectric effects on the optical process in advanced materials and devices. *Adv. Mater.* **30**(34), 1707007 (2018)
9. M.S.S. Bafqi, R. Bagherzadeh, M. Latifi, Fabrication of composite PVDF-ZnO nanofiber mats by electrospinning for energy scavenging application with enhanced efficiency. *J. Polym. Res.* **22**(7), 130 (2015)
10. Y. Zou, L. Bo, Z. Li, Recent progress in human body energy harvesting for smart bioelectronic system. *Fundame Res* **21**, 3806 (2021)
11. G. Zandesh et al., Piezoelectric electrospun nanofibrous energy harvesting devices: influence of the electrodes position and finite variation of dimensions. *J. Ind. Text.* **47**(3), 348–362 (2017)
12. M.T. Todaro et al., Biocompatible, flexible, and compliant energy harvesters based on piezoelectric thin films. *IEEE Trans. Nanotechnol.* **17**(2), 220–230 (2018)
13. Bafqi, M.S., et al., Expected lifetime of fibrous nanogenerator exposed to cyclic compressive pressure. 2020: p. 1528083720915835.
14. A. Gomez et al., Piezo-generated charge mapping revealed through direct piezoelectric force microscopy. *Nat. Commun.* **8**(1), 1–10 (2017)
15. Y. Zhang et al., Enhanced pyroelectric and piezoelectric properties of PZT with aligned porosity for energy harvesting applications. *J. Mater. Chem. A* **5**(14), 6569–6580 (2017)
16. M. Habib et al., Enhanced piezoelectric performance of donor La<sup>3+</sup>-doped BiFeO<sub>3</sub>-BaTiO<sub>3</sub> lead-free piezoceramics. *Ceram. Int.* **46**(6), 7074–7080 (2020)
17. Gao, J. et al., Recent progress on BaTiO<sub>3</sub>-based piezoelectric ceramics for actuator applications in Actuators. 2017. Multidisciplinary Digital Publishing Institute.
18. Azimi, B. et al., Electrospinning piezoelectric fibers for bio-compatible devices. *Adv Healthcare Mat.* 2019: p. 1901287.
19. Azimi, B. et al., Electrospun ZnO/poly (vinylidene fluoride-trifluoroethylene) scaffolds for lung tissue engineering. 2020(ja).
20. S. Tiwari et al., Enhanced piezoelectric response in nanoclay induced electrospun PVDF nanofibers for energy harvesting. *Energy Harvest. Syst.* **171**, 485–492 (2019)
21. S.M. Damaraju et al., Structural changes in PVDF fibers due to electrospinning and its effect on biological function. *Biomed. Mater.* **8**(4), 045007 (2013)
22. S. Gee, B. Johnson, A. Smith, Optimizing electrospinning parameters for piezoelectric PVDF nanofiber membranes. *J. Membr. Sci.* **563**, 804–812 (2018)
23. S. Gowthaman et al., A review on energy harvesting using 3D printed fabrics for wearable electronics. *J. Inst. Eng.* **99**(4), 435–447 (2018)
24. G. Zhang et al., Harvesting energy from human activity: ferroelectric energy harvesters for portable, implantable, and biomedical electronics. *Energy Technol.* **6**(5), 791–812 (2018)
25. L. Ruan et al., Properties and applications of the  $\beta$  phase poly (vinylidene fluoride). *Polymers* **10**(3), 228 (2018)
26. S. Khalid et al., A review of human-powered energy harvesting for smart electronics: Recent progress and challenges. *Int. J. Precis. Eng. Manuf.-Green Technol.* **6**(4), 821–851 (2019)
27. A. Talbourdet et al., 3D interlock design 100% PVDF piezoelectric to improve energy harvesting. *Smart Mater. Struct.* **27**(7): 075010 (2018)
28. T. Park et al., Highly conductive PEDOT electrodes for harvesting dynamic energy through piezoelectric conversion. *J. Mater. Chem. A* **2**(15), 5462–5469 (2014)
29. J. Zhao, Z. You, A shoe-embedded piezoelectric energy harvester for wearable sensors. *Sensors* **14**(7), 12497–12510 (2014)
30. D. Chen, T. Sharma, J.X. Zhang, Mesoporous surface control of PVDF thin films for enhanced piezoelectric energy generation. *Sens. Actuators A* **216**, 196–201 (2014)
31. S. Jana et al., The influence of hydrogen bonding on the dielectric constant and the piezoelectric energy harvesting performance of hydrated metal salt mediated PVDF films. *Phys. Chem. Chem. Phys.* **17**(26), 17429–17436 (2015)
32. J.-H. Lee et al., Highly sensitive stretchable transparent piezoelectric nanogenerators. *Energy Environ. Sci.* **6**(1), 169–175 (2013)
33. Y. Cho et al., Enhanced energy harvesting based on surface morphology engineering of P (VDF-TrFE) film. *Nano Energy* **16**, 524–532 (2015)
34. Z. Pi et al., Flexible piezoelectric nanogenerator made of poly (vinylidene fluoride-co-trifluoroethylene)(PVDF-TrFE) thin film. *Nano Energy* **7**, 33–41 (2014)
35. V. Bhavanasi et al., Enhanced piezoelectric energy harvesting performance of flexible PVDF-TrFE bilayer films with graphene oxide. *ACS Appl. Mater. Interfaces* **8**(1), 521–529 (2016)

36. M. Nuawi et al., Comparative study of whole-body vibration exposure between train and car passengers: a case study in malaysia. *Int. J. Automot. Mech. Eng.* **4**, 490–503 (2011)
37. A. Ismail et al., Whole-body vibration exposure of Malaysian taxi drivers. *Int. J. Automot. Mech. Eng.* **11**, 2786 (2015)
38. Mineto, A., et al., Modelling of a cantilever beam for piezoelectric energy harvesting. In: 9th Brazilian conference on Dynamics, control and their applications, Sao Carlos, 2010.
39. A.G. Muthalif, N.D. Nordin, Optimal piezoelectric beam shape for single and broadband vibration energy harvesting: Modeling, simulation and experimental results. *Mech. Syst. Signal Process.* **54**, 417–426 (2015)
40. M. Salim et al., New simulation approach for tuneable trapezoidal and rectangular piezoelectric bimorph energy harvesters. *Microsyst. Technol.* **23**(6), 2097–2106 (2017)
41. H.-C. Song et al., Multilayer piezoelectric energy scavenger for large current generation. *J. Electroceram.* **23**(2–4), 301 (2009)
42. Zhu, D., et al., A bimorph multi-layer piezoelectric vibration energy harvester. 2010.
43. M.S. Woo et al., Study on increasing output current of piezoelectric energy harvester by fabrication of multilayer thick film. *Sens. Actuators A* **269**, 524–534 (2018)
44. Y. Bai, H. Jantunen, J. Juuti, Energy harvesting research: the road from single source to multisource. *Adv. Mater.* **30**(34), 1707271 (2018)
45. D.-J. Shin et al., Multi-layered piezoelectric energy harvesters based on PZT ceramic actuators. *Ceram. Int.* **41**, S686–S690 (2015)
46. M. Safaei, H.A. Sodano, S.R. Anton, A review of energy harvesting using piezoelectric materials: state-of-the-art a decade later (2008–2018). *Smart Mater. Struct.* **28**(11), 113001 (2019)
47. W.-S. Jung et al., Powerful curved piezoelectric generator for wearable applications. *J. Nano Energy* **13**, 174–181 (2015)
48. K.-I. Park et al., Piezoelectric BaTiO<sub>3</sub> thin film nanogenerator on plastic substrates. *Nano Lett.* **10**(12), 4939–4943 (2010)
49. Bagherzadeh, R., et al., Flexible and stretchable nanofibrous piezo-and triboelectric wearable electronics.
50. Z. Yang et al., High-performance piezoelectric energy harvesters and their applications. *Joule* **2**(4), 642–697 (2018)
51. S. Paquin, Y. St-Amant, Improving the performance of a piezoelectric energy harvester using a variable thickness beam. *Smart Mater. Struct.* **19**(10), 105020 (2010)
52. Nguyen Thai, C., et al., On the nanoscale mapping of the mechanical and piezoelectric properties of poly (L-Lactic Acid) electrospun nanofibers. 2020.
53. S. Satapathy et al., Effect of annealing on phase transition in poly (vinylidene fluoride) films prepared using polar solvent. *Bull. Mater. Sci.* **34**(4), 727 (2011)
54. L. Persano et al., High performance piezoelectric devices based on aligned arrays of nanofibers of poly (vinylidene-fluoride-co-trifluoroethylene). *Nat. Commun.* **4**, 1633 (2013)
55. M.-H. You et al., A self-powered flexible hybrid piezoelectric–pyroelectric nanogenerator based on non-woven nanofiber membranes. *J. Mater. Chem. A* **6**(8), 3500–3509 (2018)
56. A. Hartono et al., Effect of mechanical treatment temperature on electrical properties and crystallite size of PVDF Film. *Adv. Mater. Phys. Chem.* **3**(1), 71–76 (2013)
57. J.I. Langford, A. Wilson, Scherrer after sixty years: a survey and some new results in the determination of crystallite size. *J. Appl. Crystallogr.* **11**(2), 102–113 (1978)

**Publisher's Note** Springer Nature remains neutral with regard to jurisdictional claims in published maps and institutional affiliations.